Plant Molecular Biology (2020) 104:615–628
https://doi.org/10.1007/s11103-020-01064-1

miR164-targeted *TaPSK5* encodes a phytosulfokine precursor that regulates root growth and yield traits in common wheat (*Triticum aestivum* L.)

Yuke Geng[1,2] · Chao Jian[1] · Wu Xu[1] · Hong Liu[1] · Chenyang Hao[1] · Jian Hou[1] · Hongxia Liu[1] · Xueyong Zhang[1] · Tian Li[1]

Received: 4 March 2020 / Accepted: 27 August 2020 / Published online: 23 September 2020

Abstract

Key message ***TaPSK5* is a less conserved target of miR164 in wheat encoding a positive regulator of root growth and yield traits that could be used for crop improvement.**

Abstract MicroRNAs (miRNAs) play key roles in regulating plant growth and development by targeting the mRNAs of conserved genes. However, little is known about the roles of less conserved miRNA-targeted genes in plants. In the current study, we identified *TaPSK5*, encoding a phytosulfokine precursor, as a novel target of miR164. Compared with miR164-targeted NAC transcription factor genes, *TaPSK5* is less conserved between monocots and dicots. Expression analysis indicated that *TaPSK5* homoeologs were constitutively expressed in wheat tissues, especially young spikes. Overexpression of *TaPSK5-D* and miR164-resistant *TaPSK5-D* (*r-TaPSK5-D*) led to increased primary root growth and grain yield in rice, with the latter having more significant effects. Comparison of the transcriptome between wild-type and *r-TaPSK5-D* overexpression plants revealed multiple differentially expressed genes involved in hormone signaling, transcription regulation, and reactive oxygen species (ROS) homeostasis. Moreover, we identified three *TaPSK5-A* haplotypes (*TaPSK5-A-Hap1/2/3*) and two *TaPSK5-B* haplotypes (*TaPSK5-B-Hap1/2*) in core collections of Chinese wheat. Both *TaPSK5-A-Hap1* and *TaPSK5-B-Hap2* are favorable haplotypes associated with superior yield traits that were under positive selection during wheat breeding. Together, our findings identify miR164-targeted *TaPSK5* as a regulator of root growth and yield traits in common wheat with potential applications for the genetic improvement of crops.

Keywords miR164 · *TaPSK5* · Root growth · Yield traits · Haplotype analysis · Wheat

Yuke Geng and Chao Jian contributed equally to this article.

Electronic supplementary material The online version of this article (https://doi.org/10.1007/s11103-020-01064-1) contains supplementary material, which is available to authorized users.

✉ Xueyong Zhang
zhangxueyong@caas.cn

✉ Tian Li
litian@caas.cn

Yuke Geng
gengyuke_321@sina.com

Chao Jian
jianchao886699@163.com

Wu Xu
1285517656@qq.com

Hong Liu
liuhyn100615@sina.com

Chenyang Hao
haochenyang@caas.cn

Jian Hou
houjian@caas.cn

Hongxia Liu
liuhongxia02@caas.cn

[1] Key Laboratory of Crop Gene Resources and Germplasm Enhancement, Institute of Crop Sciences, Chinese Academy of Agricultural Sciences, Beijing 100081, China

[2] College of Life and Environmental Science, Minzu University of China, Beijing 10081, China

Introduction

MicroRNAs (miRNAs) are a class of abundant endogenous single-stranded small RNAs (~ 21 nt) produced from noncoding, imperfectly complementary (stem-loop) RNA precursors whose biogenesis involves a complex, multistep enzymatic process (Park et al. 2005; Voinnet 2009; Rogers and Chen 2013). miRNAs play important roles in regulating plant growth and development, signal transduction, protein degradation, and responses to environmental stress and pathogen invasion (Shukla et al. 2008; Chen 2009; Voinnet 2009; Song et al. 2019). The main function of miRNAs is to negatively regulate gene expression at the transcriptional and posttranscriptional levels, including mRNA cleavage, translational repression, and epigenetic modification (Voinnet 2009; Shivram et al. 2019). With the development of high-throughput sequencing techniques, an increasing number of plant miRNAs have been identified, most of which are unique and nonconserved (Fahlgren et al. 2007; Cuperus et al. 2011). However, the bulk of studies to date have focused on highly conserved miRNAs whose functions have been broadly maintained throughout plant evolution, with fundamental roles in regulating numerous cellular events (Willmann and Poethig 2007).

The miR164 family (miR164a, miR164b, and miR164c; hereafter referred to as miR164) is a highly conserved miRNA family that functions in various biological processes, including boundary establishment and maintenance, organ formation, lateral root development, age-dependent cell death, and resistance to biotic and abiotic stresses (Laufs et al. 2004; Mallory et al. 2004; Guo et al. 2005; Fang et al. 2014; Feng et al. 2014). miR164 targets a class of NAC (NAM, ATAF, and CUC) transcription factors containing a sequence complementary to miR164 with few mismatches. The miR164-NAC module is highly conserved across plant species. In *Arabidopsis thaliana*, miR164 constricts the expansion of the boundary domain by inducing the posttranscriptional downregulation of *CUC1* and *CUC2* at the mRNA level (Laufs et al. 2004). Moreover, miR164-guided cleavage of *NAC1* mRNA provides a homeostatic mechanism that attenuates auxin signaling to regulate lateral root development (Guo et al. 2005). Overexpressing miR164-targeted NAC transcription factor genes have negative effects on drought resistance in rice at the reproduction stage (Fang et al. 2014), whereas overexpressing miR164b-resistant *OsNAC2* improves plant architecture and increases grain yields (Jiang et al. 2018). *NAC21/22* encodes a miR164-target NAC transcription factor that negatively regulates stripe rust resistance in wheat (Feng et al. 2014). Because the biological functions of miRNAs are closely related to the functions of their target genes, identifying additional targets of miR164 should help uncover complex miR164-mediated regulatory mechanisms.

Phytosulfokine (PSK) is a disulfated pentapeptide hormone that regulates cell proliferation and elongation in plants (Matsubayashi and Sakagami 2006). PSK is synthesized from approximately 80-amino-acid precursor polypeptides through posttranslational sulfation and proteolytic processing (Yang et al. 1999; Srivastava et al. 2008). Increasing evidence indicates that PSK plays fundamental roles in plant growth, development, and immunity in both dicot and monocot plants (Sauter 2015). PSK signaling promotes callus growth by inducing cell proliferation (Yang et al. 1999) and enhances root growth and hypocotyl elongation, primarily by promoting cell elongation (Kutschmar et al. 2009; Stuhrwohldt et al. 2011). Overexpression of *GhPSK* in cotton promotes fiber elongation, leading to the production of longer and finer cotton fibers (Han et al. 2014). PSK signaling also regulates plant immunity by attenuating the pathogen-associated molecular pattern (PAMP) response to bacterial pathogens (Igarashi et al. 2012; Mosher et al. 2013). Therefore, PSK signaling integrates growth and immune responses to meet the competing metabolic challenges that arise during plant development (Sauter 2015).

We previously identified *TaPSK5*, a wheat gene encoding a PSK precursor, as a potential target of miR164 based on miRNAome and degradome sequencing of developing wheat grains (Li et al. 2015). In the current study, we verified the miR164-mediated cleavage of *TaPSK5* mRNA through rapid amplification of 5′ cDNA ends (5′ RACE). Overexpressing *TaPSK5-D* and miR164-resistant *TaPSK5-D* (*rTaPSK5-D*) promoted primary root growth and improved yield traits in rice, including grain number and grain weight. We developed molecular markers based on polymorphisms in *TaPSK5-A* and *TaPSK5-B*. Haplotype analysis indicated that favorable haplotypes of *TaPSK5-A* and *TaPSK5-B* were associated with higher grain yields in natural populations of Chinese wheat. Our findings provide new insights into the miR164-PSK regulatory network and highlight the potential use of *TaPSK5* for crop improvement.

Materials and methods

Prediction and verification of miR164 target genes

Targets of miR164 were predicted using the psRNATarget program (http://plantgrn.noble.org/psRNATarget/) based on a *Triticum aestivum* cDNA library (EnsemblPlant, release 43). A four-mismatch cutoff was used to filter predicted miR164 targets, with a G–U bond counted as a 0.5 mismatch (Li et al. 2011). To map the cleavage sites in target mRNAs, RNA ligase-mediated 5′ RACE was performed

using a FirstChoice RLM-RACE Kit (Thermo Fisher Scientific, Waltham, MA, USA) according to the manufacturer's instructions. Gene-specific primers used for 5′ RACE are listed in Supplementary Table S1.

RNA extraction and quantitative reverse-transcription PCR (qRT-PCR)

Total RNA was extracted from plant materials using Tiangen RNAplant plus Reagent (Tiangen Biotech, Beijing, China). The cDNA was synthesized using a FastQuant RT Kit (Tiangen Biotech, Beijing, China). qRT-PCR analysis was performed on a LightCycler 96 real-time PCR system (Roche Applied Science, Germany) using SYBR Premix Ex Taq (Takara Bio, Beijing, China). The wheat *Actin* gene was used as the internal reference (Li et al. 2015). miRNA expression was quantified by qRT-PCR using a miRcute miRNA first-strand cDNA synthesis kit (Tiangen Biotech, Beijing, China). Relative gene expression levels (presented as fold-change values) were calculated using the comparative CT method (Livak and Schmittgen 2001). All primers are listed in Supplementary Table S1.

Vector construction and plant transformation

The coding sequences (CDSs) of *TaPSK5-A* and *TaPSK5-D* were amplified from Chinese Spring wheat cDNA and cloned into the binary vector pCAMBIA3301 under the control of the CaMV 35S promoter. The recombinant constructs were transformed into *Arabidopsis thaliana* (ecotype Col-0) by the floral-dip method using *Agrobacterium tumefaciens* GV3101. Positive transgenic plants were screened by spraying with Basta (0.1% solution). *Arabidopsis* plants were planted into small pot with soil and grown in a controlled growth chamber at 22 °C, with a 16 h light /8 h dark photoperiod, light intensity of 120 mmol m^{-2} s^{-1}, and 70% relative humidity.

To construct the *TaPSK5* overexpression vector for rice transformation, the CDS of *TaPSK5-D* was cloned into a modified pCAMBIA2300 vector under the control of the rice *ACTIN1* promoter (Liu et al. 2005). To obtain the miR164-resistant *TaPSK5-D* (*rTaPSK5-D*), mutations were introduced into the miR164 binding site of the *TaPSK5-D* CDS by PCR-mediated mutagenesis. To construct the miR164-overexpression vector, a 620-bp stem-loop precursor sequence of miR164 was amplified from wheat genomic DNA and cloned into the pCAMBIA2300 vector in a similar manner. The resulting overexpression constructs were mobilized into *Agrobacterium tumefaciens* strain EHA105 and transformed into rice (*Oryza sativa* L. ssp. *japonica*) cv. Kitaake as described (Hiei et al. 1994). Positive T_3 generations of transgenic lines were grown in the Chinese Academy of Agricultural Sciences (CAAS) experimental field (Beijing, China) for phenotypic assessment.

Phenotypic analysis

For *Arabidopsis* root length assay, seeds of wild-type (Col-0) and transgenic plants were sown on MS agar medium at 4 °C for 2.5 days and then incubated in a growth chamber at 22 °C for 3 days. The resulting seedlings were transferred to new MS plates and grown vertically for 5 days. For phenotypic analysis of rice roots, wild-type (WT) and transgenic plants were grown hydroponically at the seedling stage. In brief, three days after germination, the seedlings were transferred to plastic pots containing 1 L Hoagland nutrient solution and grown for 14 days at 25 °C in a controlled growth chamber under a 16 h/8 h light/dark photoperiod and 70% relative humidity. Hoagland solution was supplied every 3 days to provide nutrients to the seedlings. Root length was measured in at least 30 plants per line. For yield trait analysis, WT and transgenic rice plants were grown in the CAAS experimental field and observed at the maturity stage. Yield traits including panicle length, grain number, thousand-grain weight, and grain size were measured as described (Li et al. 2016).

Transient assay of miRNA–target interactions in *Nicotiana benthamiana* leaves

As described previously (Liu and Axtell 2015), a transient assay was performed to quantify miR164-mediated target repression in *N. benthamiana* leaves using a dual-luciferace reporter system with some modifications. Briefly, reporter and effector plasmids were both derived from a modified pCAMBIA1300 vector containing a CaMV 35S promoter (Chen et al. 2008). The CDSs encoding firefly luciferase (LUC) and *Renilla* luciferase (REN) were cloned into pCAMBIA1300 vector to construct 35S-LUC and 35S-REN vectors. Similarly, the miR164 precursor was cloned into pCAMBIA1300 to construct 35S-miR164 vector. Two unique restriction sites (*Bam*HI and *Sal*I) embedded in the 3′ UTR of *LUC* facilitated cloning of potential miR164 target sites. Oligos of target sites from *TaNAC92* and *TaPSK5* were inserted into the 3′ UTR of *LUC* to construct corresponding reporter plasmids. Four-week-old *N. benthamiana* leaves were infiltrated by *Agrobacterium tumefaciens* carrying 35S-miR164, 35-LUC-reporter, and 35S-REN (ratio 4:1:0.5). The relative LUC activities (LUC/REN) were measured at 72 h after infiltration using the Dual-Luciferase Reporter Assay System on a GloMax-Multi luminescence reader (Promega, Madison, WI, USA).

Transcriptome analysis

Total RNA was isolated from roots of 2-week-old rice seedlings from WT and *rTaPSK5-D* overexpression plants using Trizol reagent according to manufacturer's instructions (Invitrogen). For each genotype, 1-g root sample was collected for RNA extraction and pooled for each of the two biological replicates. Library construction and sequencing were carried out commercially on the Illumina Hiseq Novaseq platform at Kaitai Mingjing Genetech Corporation (Beijing, China). After raw sequence processing, clean reads were then mapped to the *Oryza sativa* reference genome using the HISAT2 program. The expression level of each gene was normalized by fragments per kilobase of transcript per million fragments (FKPM) using StringTie (Pertea et al. 2015). Differential expression analyses between the samples were performed using DESeq2 (Love et al. 2014). Differentially expressed genes between sample libraries were identified based on the threshold with fold-change > 2 or < 0.5, P value < 0.05, and FDR < 0.05.

Haplotype analysis of *TaPSK5* homoeologs

Thirty-six wheat accessions (24 modern cultivars and 12 landraces) were initially chosen to detect *TaPSK5* polymorphisms (Ma et al. 2016). Genome-specific primers were designed to amplify the genomic regions of three *TaPSK5* homoeologs (Table S1). The resulting DNA fragments were purified and sequenced on an ABI 3730XI DNA analyzer (Applied Biosystems). Sequence alignments were performed with DNAMAN (http://www.lynnon.com/), and sequence variations (SNPs and InDels) were identified using DNASTAR (http://www.dnastar.com/). Molecular markers were developed based on the InDels located in the *TaPSK5-A* and *TaPSK5-B* promoters. The PCR products were separated by polyacrylamide gel electrophoresis and detected by silver staining to distinguish fragment lengths.

Marker screening and haplotype association analysis were performed using 505 Chinese wheat accessions, including 157 landraces and 348 modern cultivars from core collections of Chinese wheat (Liu et al. 2020). Agronomic trait data for these wheat accessions were collected in three environments: Luoyang in Henan Province in 2002 and 2005, and Shunyi in Beijing in 2010. Phenotypic differences between haplotypes were determined by one-way analysis of variance (ANOVA) and a Tukey test at a significance level of $P < 0.05$.

Results

TaPSK5 is a less conserved target of miR164

Our previous degradome analysis identified *TaPSK5* as a new target of miR164 in wheat (Li et al. 2015). To further explore potential miR164 targets in wheat, we performed a bioinformatics search on the psRNATarget web server based on *Triticum aestivum* cDNA sequences (EnsemblPlant, release 43). As shown in Supplementary Table S2, five NAC transcription factors were predicted to be miR164 targets, which is consistent with the finding that the miR164-NAC regulatory module is highly conserved. *TaNAC92* is a representative NAC family target of miR164 whose homologs in monocots and dicots all contain highly conserved miR164-binding sites (Fig. 1a). *TaPSK5* homoeologs were also predicted to be miR164 targets, with a slight increase in the number of mismatches in the miR164 complementary sites (3.0–4.0 mismatches). Unlike highly conserved NAC targets, *TaPSK5* homologs in monocots and dicots are divergent in the miR164 binding regions (Fig. 1b). Phylogenetic analysis of PSK precursor polypeptides from *Arabidopsis*, rice, and wheat showed that potential miR164 targets including TaPSK5, OsPSK5, and OsPSK2 were classified in the same subclade (Fig. S1). Allowing for a four-mismatch cutoff, our results suggest that miR164-mediated regulation of *TaPSK5* and its homologs may be restricted to only a few monocot plants including *Triticeae*, *Oryza sativa*, and *Brachypodium*. Therefore, *TaPSK5* is a less conserved target of miR164 compared with NAC family targets.

To verify the finding that the predicted NAC genes as well as *TaPSK5* are direct targets of miR164 in wheat, we identified the cleavage sites in two genes (*TaNAC92* and *TaPSK5*) by 5′ RACE analysis. The miR164-mediated cleavage products of *TaNAC92* and *TaPSK5* mRNAs were successfully detected (Fig. 1c, d). *TaNAC92* mRNA had a very high frequency (10/10) of cleavage at the predicted position (10th nucleotide) of the miR164 binding site, whereas *TaPSK5* mRNA had a low frequency (2/15) of canonical cleavage, suggesting that miR164-mediated cleavage of *TaNAC92* mRNA is more efficient than that of *TaPSK5* mRNA. To further verify miR164–target interactions in vivo, we constructed reporter plasmids containing miR164 target sites in the 3′ UTR of a constitutively expressed LUC gene (Fig. 2a). Transient assays by co-expressing miR164 and LUC reporters in *N. benthamiana* leaves confirmed that miR164 could mediate expression repression of *TaNAC92* and *TaPSK5-D*, leading to approximately 48% and 30% decreases in relative LUC activities, respectively (Fig. 2b). In contrast, co-expression of miR164 did not cause significant expression differences of *SbPSK5* and *AtPSK6*, probably due to more mismatches in the miR164 binding regions (Figs. 1b and 2b).

Temporal and spatial expression patterns of *TaPSK5* homoeologs

To characterize *TaPSK5* and explore its potential biological function, we analyzed the spatial and temporal expression

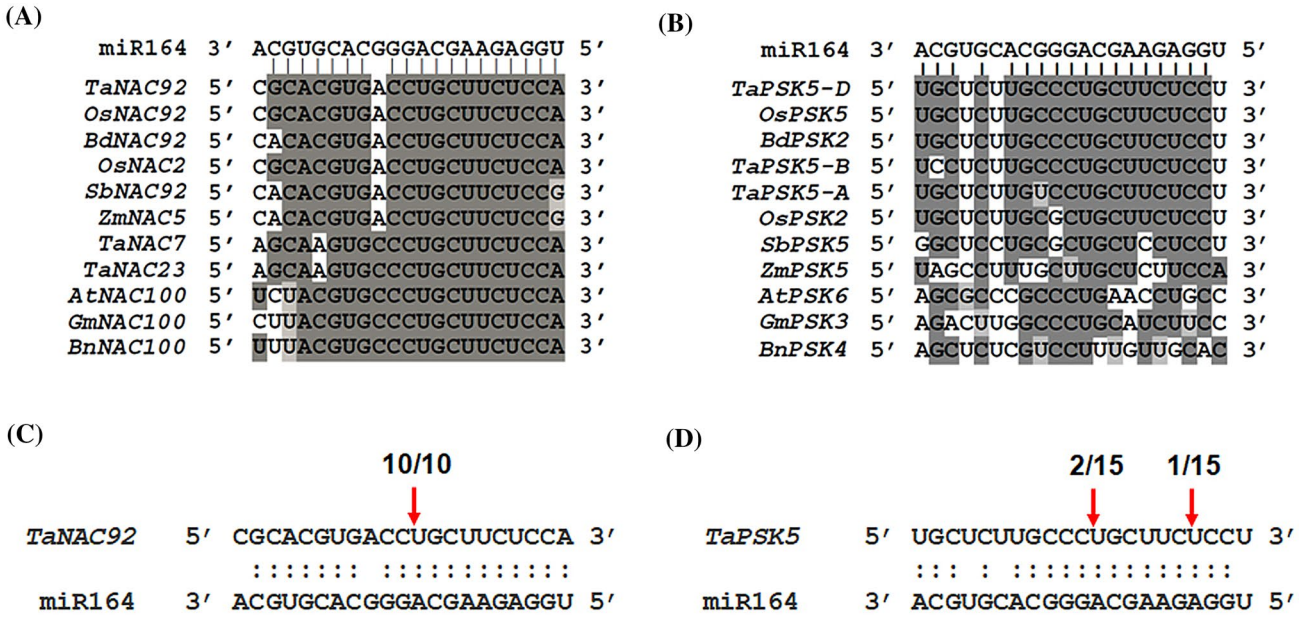

Fig. 1 miR164 targets *TaNAC92* and *TaPSK5* in wheat. **a**, **b** Sequence alignments of the miR164 binding sites of *TaNAC92* homologs (**a**) and *TaPSK5* homologs (**b**) in monocots and dicots. **c, d** Mapping of *TaNAC92* (**c**) and *TaPSK5* (**d**) mRNA cleavage sites by 5′ RACE. Arrows indicate cleavage sites, and numbers indicate the frequency of clones sequenced

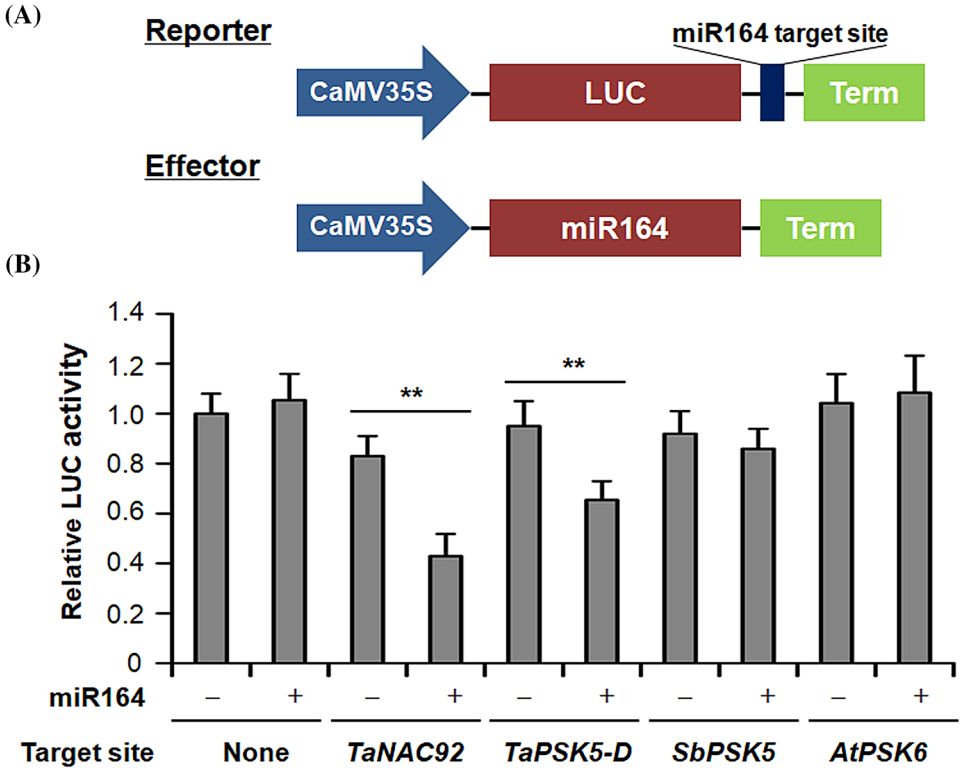

Fig. 2 miR164-mediated expression repression of *TaNAC92* and *TaPSK5* in *N. benthamiana* leaves. **a** Schematic diagram of reporter and effector constructs in dual-luciferase transient expression system. 'Term' indicates *RBS-S* terminator. **b** Transient assay by co-expression of miR164 and LUC reporters fused with potential miR164 target sites in *N. benthamiana* leaves. Target sites derived from the miR164 binding regions of *TaNAC92*, *TaPSK5*, *SbPSK5*, and *AtPSK6*. Empty vector was used as negative control (–). The relative LUC activities were measured at 72 h after infiltration. Values presented as mean ± standard deviation (SD) of five independent replicates. $^{**}P < 0.01$ (ANOVA)

patterns of *TaPSK5* homoeologs in Chinese Spring wheat by performing qRT-PCR with genome-specific primers (Supplementary Table S1). As shown in Fig. 3, all *TaPSK5* homoeologs were constitutively expressed in wheat tissues such as roots, leaves, and stems at the seedling stage or heading stage, but they were expressed at higher levels in developing young spikes. The *TaPSK5* homoeologs were expressed at higher levels in younger spikes or grains during

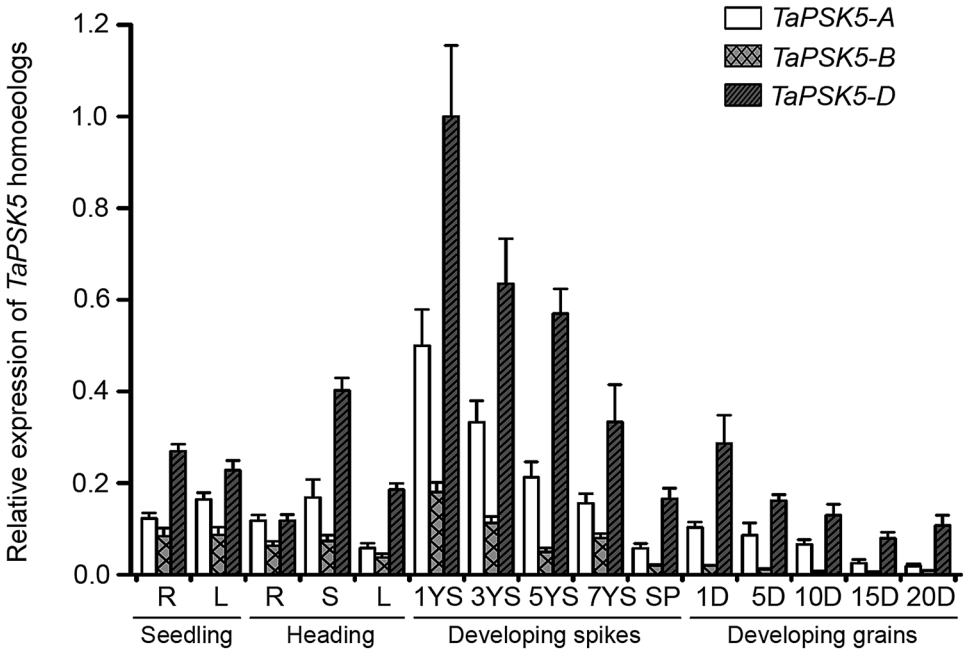

Fig. 3 Temporal and spatial expression patterns of *TaPSK5* homoeologs in wheat. *R* root, *L* leaf, *S* stem, *1YS–7YS* 1–7-cm young spike, *SP* spike at heading stage, *1D–20D* grain at 1–20 days after pollination. Genome-specific primers were used for *TaPSK5* homoeologs, and the wheat *Actin* gene was used as internal reference. Relative gene expression levels were calculated using the comparative CT method. Values presented as mean ± SD of three independent replicates

spike or grain development, which is consistent with their function in promoting cell division and elongation. Although the *TaPSK5* homoeologs exhibited similar expression patterns, *TaPSK5-D* was expressed at a higher level than *TaPSK5-A* and *TaPSK5-B*, which is similar to the results in the wheat expression database (http://www.wheat-expression.com/).

Overexpression of *TaPSK5-D* and *rTaPSK5-D* promotes root growth in rice

To determine whether *TaPSK5* is a functional *PSK* gene, we generated transgenic *Arabidopsis* plants expressing *TaPSK5-A* or *TaPSK5-D* under the control of the CaMV 35S promoter. The roots of all *TaPSK5-A* and *TaPSK5-D* transgenic lines were significantly longer than those of the Col-0 control (Supplementary Fig. S2), which is consistent with the phenotypes of plants overexpressing functional *Arabidopsis PSK* genes (Yu et al. 2016).

Next, we generated *TaPSK5*- and *rTaPSK5*-overexpressing rice plants expressing *TaPSK5-D* or miR164-resistant *TaPSK5-D* (*rTaPSK5-D*) under the control of the rice *ACTIN1* promoter. For *rTaPSK5-D*, two point mutations were introduced into the miR164 binding site without altering the amino acid sequence (Fig. 4a). Transient assays in *N. benthamiana* leaves showed that the point mutations of *rTaPSK5-D* could perturb the miR164-mediated expression repression (Fig. S3). Consistently, *TaPSK5* was expressed at significantly higher levels in *rTaPSK5-D-OE* versus *TaPSK5-D-OE* plants (Fig. 4b and Supplementary Fig. S3), indicating that the miR164-resistant form of *TaPSK5-D* could result in enhanced accumulation of *TaPSK5* transcripts. Transgenic rice seedlings harboring both *TaPSK5* and *rTaPSK5* showed accelerated root growth, but the effects caused by overexpression of *rTaPSK5* were stronger (Fig. 4c). The average primary root length of *TaPSK5-OE* plants was significantly greater than that of the WT control and lower than that of *rTaPSK5-OE* plants (Fig. 4d). Therefore, *TaPSK5* encodes a positive regulator of root growth, and its regulatory effect is restricted by miR164.

We also generated miR164-overexpressing rice plants to clarify the effects of this miRNA on root growth. Compared with the WT plants, all three independent miR164 overexpression lines showed a more than one-fold increase in miR164 abundance and a corresponding decrease in *OsPSK5* transcript levels (Fig. S4), confirming the notion that both *TaPSK5* and *OsPSK5* are targets of miR164. The root lengths of miR164-overexpression plants were reduced by more than 25% compared with the WT (Fig. S4), in contrast to the phenotype observed for the *TaPSK5*-overexpression lines. However, miR164 overexpression also led to reduced shoot length (Fig. S4), whereas *TaPSK5* overexpression did not lead to altered shoot growth (Fig. 4b). These results indicate that miR164 plays a widespread role in plant development, possibly by regulating the expression of multiple targets including *NACs* and *PSK5*.

Overexpression of *TaPSK5-D* and *rTaPSK5-D* improves yield traits in rice

The finding that *TaPSK5* was expressed at high levels in developing young spikes suggests that it might also be involved in regulating yield traits. To test this hypothesis, we measured multiple yield-related traits in WT,

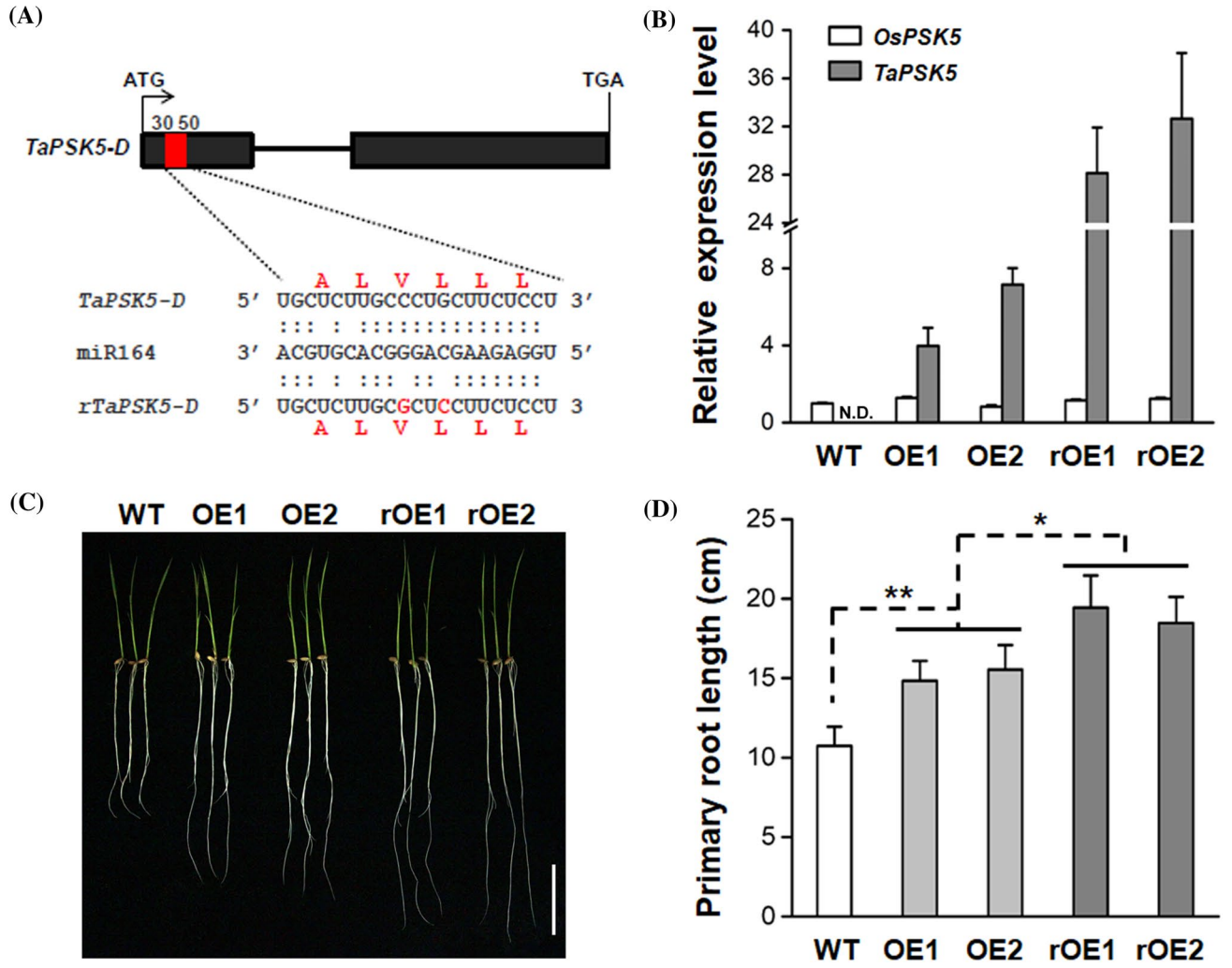

Fig. 4 Overexpression of *TaPSK5-D* and *rTaPSK5-D* promotes root growth in rice seedlings. **a** Schematic representation of the *TaPSK5-D* and *rTaPSK5-D* constructs. **b** Relative expression levels of *OsPSK5* and *TaPSK5* in 2-week-old wild-type (WT), *TaPSK5-D*-overexpression (OE), and *rTaPSK5-D*-overexpression (rOE) seedlings. Rice *Actin* gene was used as internal reference. Values presented as mean ± SD. $^{**}P < 0.01$ (ANOVA). N.D., not detectable. **c** Comparison of root growth among WT, OE, and rOE transgenic rice seedlings. Bar = 5 cm. **d** Primary root length of WT, OE, and rOE transgenic rice seedlings. $^{*}P < 0.05$ and $^{**}P < 0.01$ (ANOVA)

TaPSK5-D-OE, and *rTaPSK5-D-OE* rice plants, including plant height, tiller number, panicle length, grain number per panicle (GN), thousand-grain weight (TGW), grain length, and grain width. Although no significant differences in plant height or tiller number were observed between the WT and transgenic plants (Figs. 5a and Supplementary Fig. S5), *TaPSK5-D* and *rTaPSK5-D* plants showed better yield traits than the WT, such as longer main panicles, higher GN, larger grain size, and higher TGW (Fig. 5b–g). Notably, the increased TGW in the transgenic plants mainly resulted from an increase in grain length rather than grain width (Fig. 5g and Supplementary Fig. S5). Although the difference was not significant, the *rTaPSK5-D* plants showed slight increases in yield traits compared with *TaPSK5-D* plants (Fig. 5b–g). These results confirm the notion that overexpressing *TaPSK5-D* and *rTaPSK5-D* improves yield traits in rice.

Identification of differentially expressed genes between WT and *rTaPSK5-D-OE* by RNA-seq

To explore the possible functional mechanism of *TaPSK5* in promoting root growth, we analyzed the transcriptome of 2-week-old seedling roots of WT and *rTaPSK5-D-OE1* using RNA-SEq. Based on a $\log_2$ fold-change threshold of < -0.5 or > 0.5, with a *P* value and FDR < 0.05, a total of 348 genes were identified as differentially expressed genes between WT and *rTaPSK5-D-OE1* (Fig. S6). Compared with the WT, 240 and 148 genes were determined to be up- and downregulated, respectively, in the *rTaPSK5-D-OE1*

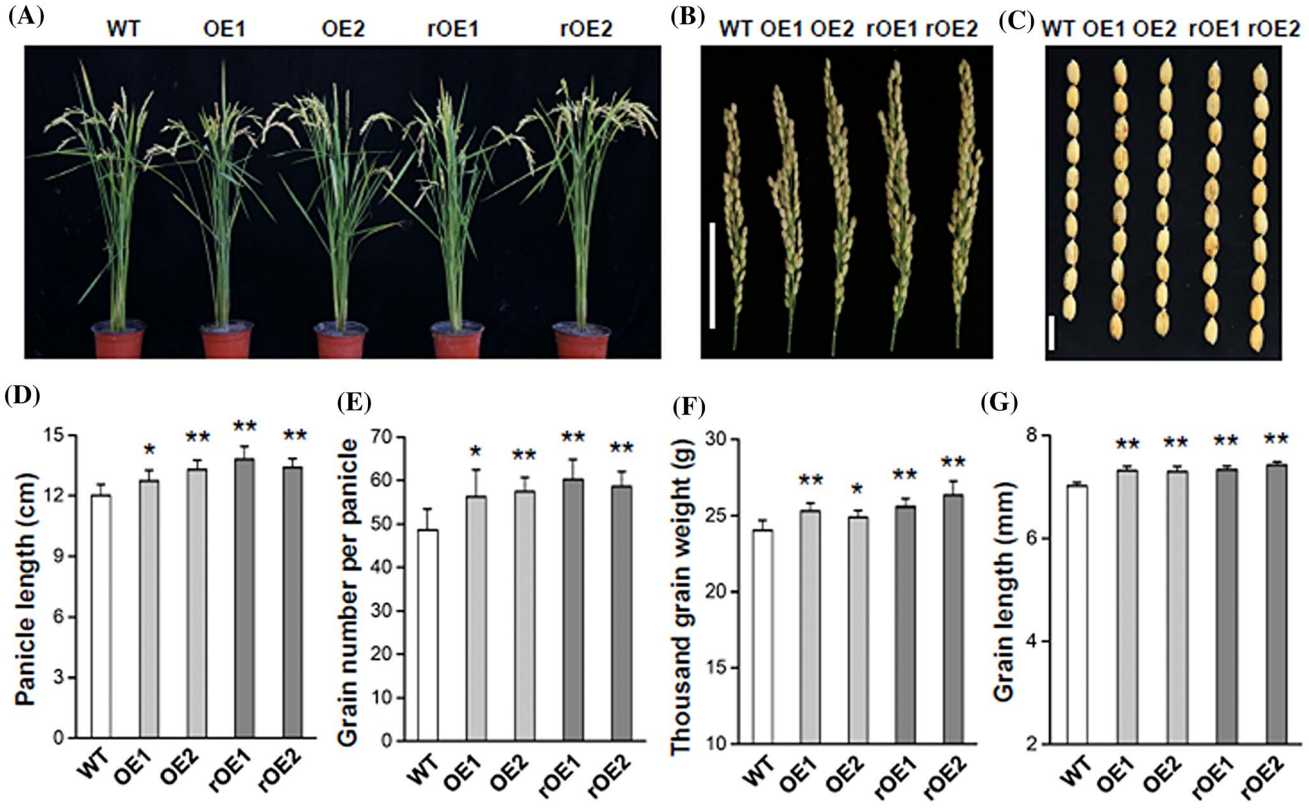

Fig. 5 Overexpression of *TaPSK5-D* and *rTaPSK5-D* improves yield traits in transgenic rice. **a–c** Phenotypic comparison of whole plants (**a**), panicles (**b**), and grains (**c**) at adult stage among wild-type (WT), *TaPSK5-D* overexpression (OE), and *rTaPSK5-D* overexpression (rOE) plants. Bar = 5 cm in **a** and bar = 1 cm in (**b**). **d–g** Panicle length (**d**), grain number per panicle (**e**), thousand-grain weight (**f**), and grain length (**g**) in WT, OE, and rOE plants. Values presented as mean ± SD. $*P < 0.05$ and $**P < 0.01$ (ANOVA) indicate significant difference from WT

line (Fig. S6). Interestingly, some hormone-related genes and transcription regulators were significantly upregulated in the *rTaPSK5-D-OE1* line. These genes were involved in brassinosteroid (BR), auxin, and jasmonate (JA) signaling and transcription regulation network, such as *OsBRI1* (BR), *OsIAA8* and *OsIAA14* (auxin), *OsJAZ9* (JA), and several NAC and HOX family transcription factors (Fig. 6a). Moreover, multiple genes encoding peroxidases were differentially expressed between WT and *rTaPSK5-D-OE1*, and most of them were upregulated in the *rTaPSK5-D-OE1* line (Fig. 6b), indicating that homeostasis of ROS might play a role in accelerating root growth in transgenic plants. We performed qRT-PCR analysis to further confirm the expression patterns of five representative genes (*OsBRI1*, *OsIAA14*, *OsJAZ9*, *OsNAC12*, and Os07g0676900) among WT, *TaPSK5-D-OE*, and *rTaPSK5-D-OE* plants. As shown in Fig. 6c, all five genes were upregulated in *TaPSK5-D-OE* and *rTaPSK5-D-OE* lines compared with the WT, consistent with our transcriptome data. Notably, only *OsBRI1* and Os07g0676900 exhibited *TaPSK5* dose-dependent effects, showing higher expression levels in *rTaPSK5-D-OE* than *TaPSK5-D-OE* lines (Fig. 6c).

Haplotype identification of *TaPSK5* homoeologs in Chinese wheat accessions

To investigate genetic effects of *TaPSK5* homoeologs and identify their favorable alleles in wheat, we sequenced the coding and promoter regions of *TaPSK5* homoeologs (*TaPSK5-A*, *-B*, and *-D*) in 36 Chinese wheat accessions and detected polymorphic sites only in the promoter regions of *TaPSK5-A* and *TaPSK5-B* (Fig. 7a, b). No variations were observed in the coding regions of *TaPSK5-A*, *-B*, or *-D*. Among promoter regions, only one simple sequence repeat (SSR) was detected in the 2.1-kb region upstream of the ATG start codon of *TaPSK5-A* (Fig. 7a), and 17 SNPs and 2 InDels were present in the 3.0-kb region upstream of the ATG start codon of *TaPSK5-B* (Fig. 7b). These variations resulted in three *TaPSK5-A* haplotypes (*TaPSK5-A-Hap1/2/3*) and two *TaPSK5-B* haplotypes (*TaPSK5-B-Hap1/2*) among the common wheat accessions examined. We developed two molecular markers based on the SSR (–249 bp) in *TaPSK5-A* and the 13-bp InDel (–2760 bp) in *TaPSK5-B* to distinguish the three *TaPSK5-A* haplotypes and two *TaPSK5-B* haplotypes, respectively (Fig. 7a, b).

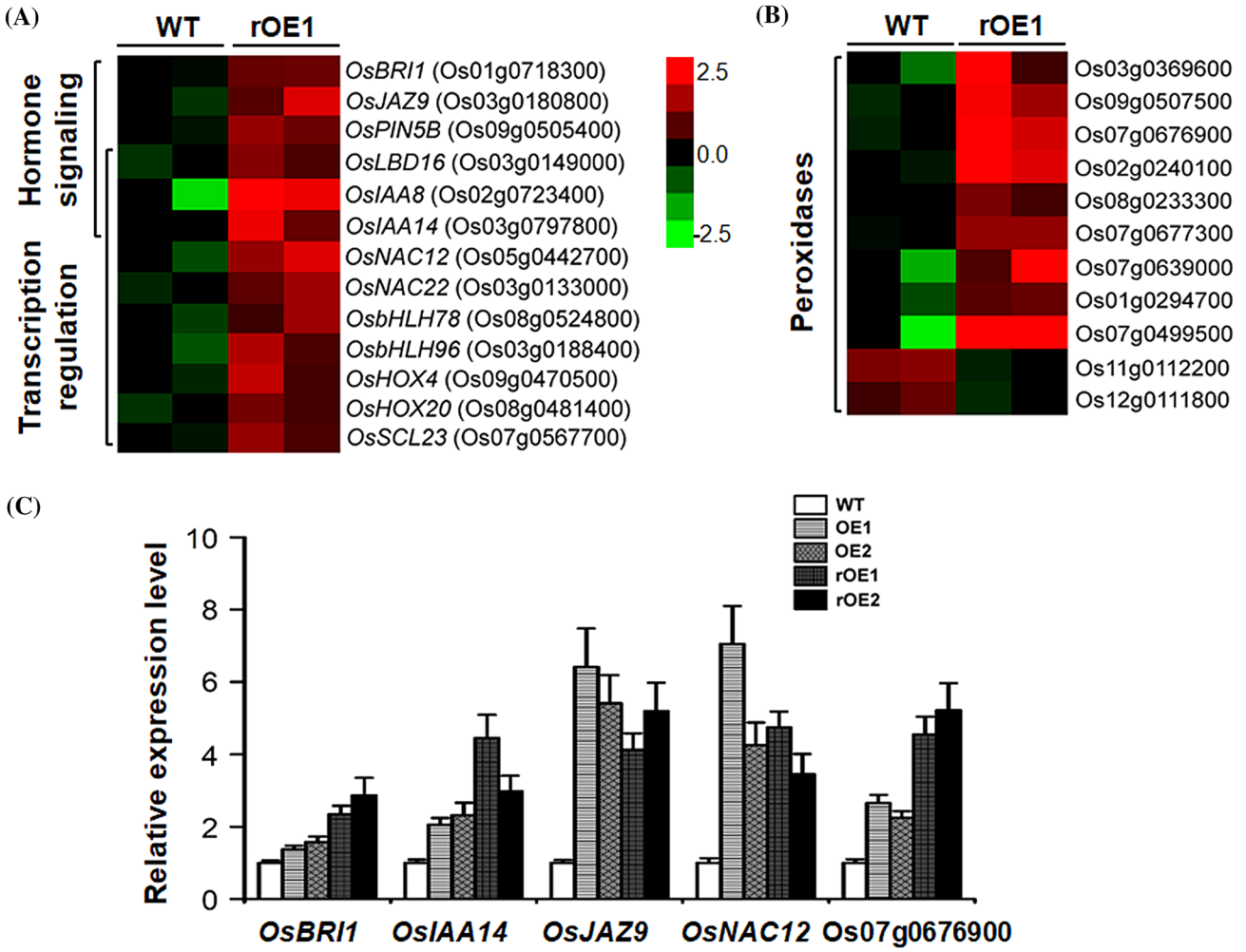

Fig. 6 Transcriptome and qPCR analysis of differentially expressed genes between WT and *rTaPSK5-D-OE1* (rOE1) line. **a** Heatmap showing that representative genes involved in hormone signaling and transcription regulation were upregulated in the rOE1. Values of $\log_2$ fold-change (rOE1/WT) are indicated in different colors (red to green). **b** Heatmap showing peroxidase-encoding genes differentially expressed between WT and rOE1. **c** Validation of five representative upregulated genes by qRT-PCR. Rice *Actin* gene was used as internal reference. Values presented as mean ± SD

TaPSK5-A and *TaPSK5-B* haplotypes were associated with yield traits in natural populations of Chinese wheat

By using the newly developed molecular markers, we genotyped 505 Chinese wheat accessions, including 157 landraces and 348 modern cultivars, from core collections of Chinese wheat. We then performed association analysis between the *TaPSK5-A*/*B* haplotypes and multiple yield traits from plants collected in three environments (2002, 2005, and 2010). Because the frequency of *TaPSK5-A-Hap3* was very low (less than 4%) in both the landraces and modern cultivars, we did not use this haplotype in the association analysis. Significant differences in GN were detected between *TaPSK5-A-Hap1* and *TaPSK5-A-Hap2* in both populations. The mean GN of *TaPSK5-A-Hap1* was 5.1–5.9 higher in the landraces and 2.4–6.3 higher in the modern cultivars compared with *TaPSK5-A-Hap2* in all three environments (Fig. 8a). Moreover, the *TaPSK5-B* haplotypes were significantly correlated with TGW in both populations. Compared with *TaPSK5-B-Hap1*, the mean TGW of *TaPSK5-B-Hap2* was 5.1–5.9 g higher in the landraces and 2.4–6.3 g higher in the modern cultivars in all three environments (Fig. 8b). These results indicate that both *TaPSK5-A-Hap1* and *TaPSK5-B-Hap2* are favorable haplotypes associated with superior yield traits, such as higher GN and higher TGW.

TaPSK5-A-Hap1 and *TaPSK5-B-Hap2* underwent positive selection during Chinese wheat breeding

Favorable haplotypes have always been subjected to positive selection during wheat breeding (Ma et al. 2016; Liu

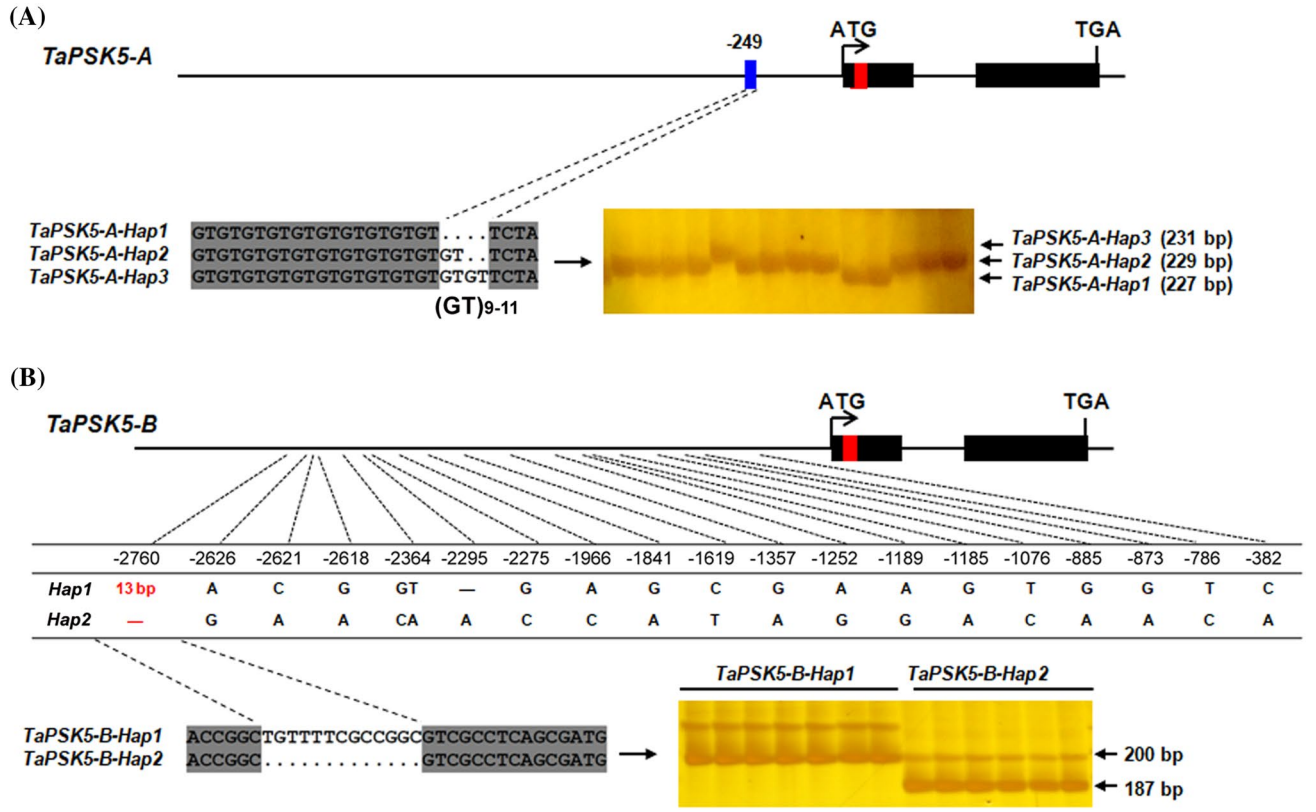

Fig. 7 Haplotype identification in common Chinese wheat accessions and development of molecular markers for *TaPSK5-A* and *TaPSK5-B*. **a** An SSR (GT repeat) located in the *TaPSK5-A* promoter region (forming three haplotypes) was used to develop a molecular marker. **b** Two InDels and 17 SNPs located in the *TaPSK5-B* promoter region (forming two haplotypes) were used to develop a molecular marker based on the 13-bp InDel

et al. 2020). We investigated the geographic distribution of *TaPSK5-A*/*B* haplotypes in both landraces and modern cultivars from China's ten ecological zones. The favorable *TaPSK5-A-Hap1* associated with high GN was subjected to weak positive selection mainly in zones I, II, and III, which are major wheat production zones in China (Fig. S7). By contrast, *TaPSK5-B-Hap1*, the high-TGW haplotype, was subjected to strong selection in almost all production zones, with an increase in frequency from 13% in landraces to 60% in modern cultivars (Fig. S7). These results indicate that both *TaPSK5-A-Hap1* and *TaPSK5-A-Hap2* were subjected to positive selection during wheat breeding, but the degree of selection pressure on these two favorable haplotypes varied in different production zones.

Discussion

In plants, most conserved miRNAs regulate highly conserved target genes involved in development and hormone signaling. Many of these target genes encode transcription factors and generally retained conserved miRNA-binding sites across plant evolution. Therefore, many miRNA-target regulatory modules comprising conserved miRNAs and their targets have been identified, such as miR156-SPLs, miR164-NACs, and miR396-GRFs (Willmann and Poethig 2007). Genome-wide analyses of miRNA targets have revealed that conserved miRNAs can also regulate targets that are not broadly conserved (Debernardi et al. 2012; Zhao et al. 2016). In *Arabidopsis*, *bHLH74* is a verified target of miR396, but *bHLH74* homologs with miR396 binding sites are only present in species within the sister families *Cleomaceae* and *Brassicaceae* (Debernardi et al. 2012). In the current study, by performing 5′ RACE, transient assay, and transgenic analysis, we determined that *TaPSK5* is a less conserved target of miR164 (Figs. 1d, 2b, and 4b–d). Indeed, *TaPSK5* homologs with miR164 binding sites are restricted to closely related monocot plants including *Triticeae*, *Oryza sativa*, and *Brachypodium* (Figs. 1b, 2b). Thus, our findings provide new evidence supporting the notion that conserved miRNAs have acquired new targets during evolution in various plant species. The identification of additional miRNA targets could help fully elucidate the specific functions of conserved miRNAs.

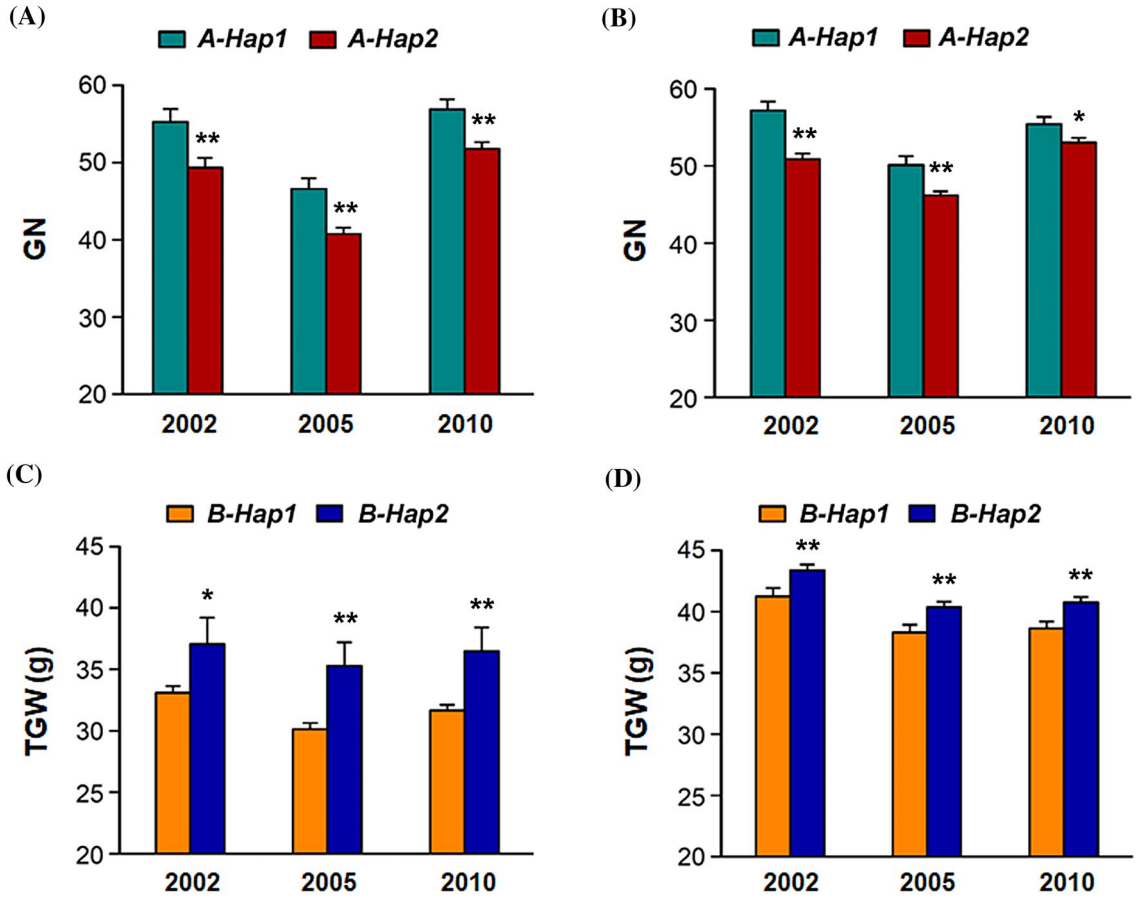

Fig. 8 Association of *TaPSK5-A* and *TaPSK5-B* haplotypes with yield traits in natural populations of Chinese wheat. **a**, **b** Association of *TaPSK5-A* haplotypes (*A-Hap*) with GN in landraces (**a**) and modern cultivars (**b**) in three environments (2002, 2005, and 2010). There were 42 and 108 *A-Hap1* and *A-Hap2* accessions among landraces (**a**) and 89 and 257 *A-Hap1* and *A-Hap2* accessions among modern cultivars (**b**), respectively. **c**, **d** Association of *TaPSK5-B* haplotypes (*B-Hap*) with TGW in both landraces (**c**) and modern cultivars (**d**) in three environments (2002, 2005. and 2010). There were 136 and 20 *B-Hap1* and *B-Hap2* accessions among landraces (**c**) and 131 and 209 *B-Hap1* and *B-Hap2* accessions among modern cultivars (**d**), respectively. Values presented as mean ± SE. $*P < 0.05$ and $**P < 0.01$ (ANOVA)

PSK signaling regulates cell proliferation and elongation in plants (Matsubayashi and Sakagami 2006). In the current study, both transgenic *Arabidopsis* and rice plants constitutively overexpressing *TaPSK5* had significantly longer roots than the WT controls (Fig. 4c and Supplementary Fig. S2), which is consistent with the finding that PSK signaling plays a conserved role in promoting root growth (Kutschmar et al. 2009). More interestingly, overexpressing *TaPSK5-D* also improved yield traits in transgenic rice, including larger panicles and grain size, higher GN, and higher TGW (Fig. 5a–g). Overexpressing miR164-resistant *TaPSK5-D* in transgenic rice plants caused more obvious increases in root growth (Fig. 4a–d), indicating that the hormone PSK may have a dose-dependent effect on plants. We believe that the yield improvement obtained by overexpressing *TaPSK5-D* mainly resulted from the role of PSK in directly regulating reproductive organ growth based on its high expression levels in young spikes and grains (Fig. 3), which can be supported by the fact that the difference in yield traits between *TaPSK5-OE* and *rTaPSK5-OE* is not as significant as that in root traits. Moreover, overexpressing *GhPSK* in cotton promoted fiber elongation and enhanced fiber quality (Han et al. 2014). These findings indicate that PSK signaling is a versatile regulator of plant growth and development and that manipulating its expression has potential applications for crop improvement.

So far, plant PSK signaling through PSKR receptors has been well established, and some crucial regulators of PSKs have been identified (Matsubayashi et al. 2002; Heyman et al. 2013). However, PSK signaling pathway is far from being fully understood downstream of perception. Our transcriptome data identified hundreds of differentially expressed genes between WT and *rTaPSK5-OE* plants (Fig. S6), which contributed to elucidate PSK signaling in

promoting root growth. Among them, a few hormone-related genes were significantly upregulated in the *rTaPSK5-OE* plants (Fig. 6a). For example, the brassinosteroid receptor *OsBRI1*, a key member in BR signaling pathway, demonstrated a *TaPSK5* dose-dependent expression pattern, with higher expression level in *rTaPSK5-OE* plants than WT and *TaPSK5-OE* plants (Fig. 6c). Previous studies have shown that plant BRI1 has structural similarity with PSKR receptors and BR mediates PSK-dependent elongation growth in roots (Hartmann et al. 2013; Ladwig et al. 2015). Our study indicated that PSK accumulation would in turn induce the expression of *BRI1* and enhance the BR signaling in root growth. In addition to BR, the plant hormone auxin (primarily indole-3-acetic acid, IAA) plays an essential role in root growth (Pacifici et al. 2015). Consistently, PSK promoted the expression of auxin-related genes including auxin efflux carrier *OsPIN5B* and auxin-responsive transcription factors *OsIAA8*, *OsIAA14*, and *OsLBD16* (Fig. 6a). Transcription factors are also important regulators of root growth (Chen et al. 2018), and PSK-induced NAC and HOX family transcription factors have potential functions in accelerating root growth downstream of PSK signaling. Moreover, ROS act as important signal molecules in controlling root growth and development (Tsukagoshi 2016). We identified multiple differentially expressed peroxidase-encoding genes, and found most of them to be upregulated in the *rTaPSK5-OE* plants (Fig. 6b), indicating a molecular link between PSK and ROS. Together, our transcriptome data reveal a complex network of interactions between PSK and other plant hormones and signal molecules.

Yield improvement is a major objective of wheat breeding programs due to the enormous demand for wheat by an increasing worldwide population. Marker-assisted selection (MAS) is a highly efficient approach for genetic yield improvement in wheat (Ma et al. 2019). In the current study, we identified three *TaPSK5-A* haplotypes and two *TaPSK5-B* haplotypes among Chinese wheat accessions and developed molecular markers to distinguish between the distinct haplotypes of *TaPSK5-A* and *TaPSK5-B* (Fig. 7a, b). Our association analysis showed that the *TaPSK5-A* and *TaPSK5-B* haplotypes were significantly correlated with GN and TGW, respectively, in both Chinese landraces and modern cultivars (Fig. 8a–d). The different genetic effects of *TaPSK5-A* and *TaPSK5-B* haplotypes point to the possible subfunctionalization of homoeologous genes, which has been reported for gene sets such as *TaCPK2* and *TaGW8* (Geng et al. 2013; Ma et al. 2019). *TaPSK5-A-Hap1* is the favorable *TaPSK5-A* haplotype associated with higher GN, and *TaPSK5-B-Hap2* is the favorable *TaPSK5-B* haplotype associated with higher TGW (Fig. 8a–d). We propose that this functional divergence resulted in differential selection pressure on *TaPSK5-A-Hap1* and *TaPSK5-B-Hap2* during Chinese wheat breeding. *TaPSK5-B-Hap2* was subjected to stronger positive selection than *TaPSK5-A-Hap1* (Fig. S7), which is consistent with the finding that TGW was the prioritized target among the three yield components during a century of wheat breeding in China (Hou et al. 2014). As combinations of favorable alleles or haplotypes usually show additive effects, pyramiding favorable haplotypes of *TaPSK5-A/B* and other yield-related genes could be highly effective for improving wheat yields in the future.

In conclusion, we identified *TaPSK5*, a less conserved target of miR164, as a novel positive regulator of root growth and yield traits in wheat. Transgenic and haplotype analyses highlighted the potential of targeting *TaPSK5* for genetic improvement in crops.

Acknowledgements This work was supported by the National Natural Science Foundation of China (31671687) and the National Animal and Plant Transgenic Project (2016ZX08009001).

Author contributions T.L. and X.Z. conceived and designed the research. Y.G., C.J., W.X., and H.L. performed the experiments. C.H., J.H., and H.L. analyzed the data. T.L., Y.G., and X.Z. wrote the manuscript.

Compliance with ethical standards

Conflict of interest All authors declare that they have no conflicts of interest.

References

Chen X (2009) Small RNAs and their roles in plant development. Annu Rev Cell Dev Biol 25:21–44

Chen H, Zou Y, Shang Y, Lin H, Wang Y, Cai R, Tang X, Zhou JM (2008) Firefly luciferase complementation imaging assay for protein-protein interactions in plants. Plant Physiol 146:368–376

Chen D, Chai S, McIntyre CL, Xue GP (2018) Overexpression of a predominantly root-expressed NAC transcription factor in wheat roots enhances root length, biomass and drought tolerance. Plant Cell Rep 37:225–237

Cuperus JT, Fahlgren N, Carrington JC (2011) Evolution and functional diversification of MIRNA genes. Plant Cell 23:431–442

Debernardi JM, Rodriguez RE, Mecchia MA, Palatnik JF (2012) Functional specialization of the plant miR396 regulatory network through distinct microRNA-target interactions. PLoS Genet 8:e1002419

Fahlgren N, Howell MD, Kasschau KD, Chapman EJ, Sullivan CM, Cumbie JS, Givan SA, Law TF, Grant SR, Dangl JL, Carrington JC (2007) High-throughput sequencing of Arabidopsis microRNAs: evidence for frequent birth and death of MIRNA genes. PLoS ONE 2:e219

Fang Y, Xie K, Xiong L (2014) Conserved miR164-targeted NAC genes negatively regulate drought resistance in rice. J Exp Bot 65:2119–2135

Feng H, Duan X, Zhang Q, Li X, Wang B, Huang L, Wang X, Kang Z (2014) The target gene of tae-miR164, a novel NAC transcription factor from the NAM subfamily, negatively regulates resistance of wheat to stripe rust. Mol Plant Pathol 15:284–296

Geng S, Li A, Tang L, Yin L, Wu L, Lei C, Guo X, Zhang X, Jiang G, Zhai W, Wei Y, Zheng Y, Lan X, Mao L (2013) *TaCPK2-A*, a

calcium-dependent protein kinase gene that is required for wheat powdery mildew resistance enhances bacterial blight resistance in transgenic rice. J Exp Bot 64:3125–3136

Guo HS, Xie Q, Fei JF, Chua NH (2005) MicroRNA directs mRNA cleavage of the transcription factor NAC1 to downregulate auxin signals for *Arabidopsis* lateral root development. Plant Cell 17:1376–1386

Han J, Tan J, Tu L, Zhang X (2014) A peptide hormone gene, *GhPSK* promotes fibre elongation and contributes to longer and finer cotton fibre. Plant Biotechnol J 12:861–871

Hartmann J, Stührwohldt N, Dahlke RI, Sauter M (2013) Phytosulfokine control of growth occurs in the epidermis, is likely to be non-cell autonomous and is dependent on brassinosteroids. Plant J 73:579–590

Heyman J, Cools T, Vandenbussche F et al (2013) ERF115 controls root quiescent center cell division and stem cell replenishment. Science 342:860–863

Hiei Y, Ohta S, Komari T, Kumashiro T (1994) Efficient transformation of rice (*Oryza sativa* L.) mediated by *Agrobacterium* and sequence analysis of the boundaries of the T-DNA. Plant J 6:271–282

Hou J, Jiang Q, Hao C, Wang Y, Zhang H, Zhang X (2014) Global selection on sucrose synthase haplotypes during a century of wheat breeding. Plant Physiol 164:1918–1929

Igarashi D, Tsuda K, Katagiri F (2012) The peptide growth factor, phytosulfokine, attenuates pattern-triggered immunity. Plant J 71:194–204

Jiang D, Chen W, Dong J, Li J, Yang F, Wu Z, Zhou H, Wang W, Zhuang C (2018) Overexpression of miR164b-resistant *OsNAC2* improves plant architecture and grain yield in rice. J Exp Bot 69:1533–1543

Kutschmar A, Rzewuski G, Stuhrwohldt N, Beemster GT, Inze D, Sauter M (2009) PSK-alpha promotes root growth in *Arabidopsis*. New Phytol 181:820–831

Ladwig F, Dahlke RI, Stührwohldt N, Hartmann J, Harter K, Sauter M (2015) Phytosulfokine regulates growth in *Arabidopsis* through a response module at the plasma membrane that includes CYCLIC NUCLEOTIDE-GATED CHANNEL17, H+-ATPase, and BAK1. Plant Cell 27:1718–1729

Laufs P, Peaucelle A, Morin H, Traas J (2004) MicroRNA regulation of the CUC genes is required for boundary size control in Arabidopsis meristems. Development 131:4311–4322

Li T, Li H, Zhang YX, Liu JY (2011) Identification and analysis of seven H_2O_2-responsive miRNAs and 32 new miRNAs in the seedlings of rice (*Oryza sativa* L. ssp. *indica*). Nucleic Acids Res 39:2821–2833

Li T, Ma L, Geng Y, Hao C, Chen X, Zhang X (2015) Small RNA and degradome sequencing reveal complex roles of miRNAs and their targets in developing wheat grains. PLoS ONE 10:e0139658

Li B, Liu D, Li Q, Mao X, Li A, Wang J, Chang X, Jing R (2016) Overexpression of wheat gene *TaMOR* improves root system architecture and grain yield in *Oryza sativa*. J Exp Bot 67:4155–4167

Liu Q, Axtell MJ (2015) Quantitating plant microRNA-mediated target repression using a dual-luciferase transient expression system. In: Alonso J, Stepanova A (eds) Plant functional genomics. Methods in molecular biology. Humana Press, New York, pp 287–303

Liu B, Li P, Li X, Liu C, Cao S, Chu C, Cao X (2005) Loss of function of *OsDCL1* affects microRNA accumulation and causes developmental defects in rice. Plant Physiol 139:296–305

Liu H, Li H, Hao C, Wang K, Wang Y, Qin L, An D, Li T, Zhang X (2020) *TaDA1*, a conserved negative regulator of kernel size, has an additive effect with *TaGW2* in common wheat (*Triticum aestivum* L.). Plant Biotechnol J 18:1330–1342

Livak KJ, Schmittgen TD (2001) Analysis of relative gene expression data using real-time quantitative PCR and the $2^{-\Delta\Delta CT}$ method. Methods 25:402–408

Love MI, Huber W, Anders S (2014) Moderated estimation of fold change and dispersion for RNA-seq data with DESeq2. Genome Biol 15:550

Ma L, Li T, Hao C, Wang Y, Chen X, Zhang X (2016) *TaGS5-3A*, a grain size gene selected during wheat improvement for larger kernel and yield. Plant Biotechnol J 14:1269–1280

Ma L, Hao C, Liu H, Hou J, Li T, Zhang X (2019) Diversity and subfunctionalization of *TaGW8* homoeologs hold potential for genetic yield improvement in wheat. Crop J 7:830–844

Mallory AC, Dugas DV, Bartel DP, Bartel B (2004) MicroRNA regulation of NAC-domain targets is required for proper formation and separation of adjacent embryonic, vegetative, and floral organs. Curr Biol 14:1035–1046

Matsubayashi Y, Sakagami Y (2006) Peptide hormones in plants. Annu Rev Plant Biol 57:649–674

Matsubayashi Y, Ogawa M, Morita A, Sakagami Y (2002) An LRR receptor kinase involved in perception of a peptide plant hormone, phytosulfokine. Science 296:1470–1472

Mosher S, Seybold H, Rodriguez P, Stahl M, Davies KA, Dayaratne S, Morillo SA, Wierzba M, Favery B, Keller H, Tax FE, Kemmerling B (2013) The tyrosine-sulfated peptide receptors PSKR1 and PSY1R modify the immunity of Arabidopsis to biotrophic and necrotrophic pathogens in an antagonistic manner. Plant J 73:469–482

Pacifici E, Polverari L, Sabatini S (2015) Plant hormone cross-talk: the pivot of root growth. J Exp Bot 66:1113–1121

Park MY, Wu G, Gonzalez-Sulser A, Vaucheret H, Poethig H (2005) Nuclear processing and export of microRNAs in *Arabidopsis*. Proc Natl Acad Sci USA 102:3691–3696

Pertea M, Pertea GM, Antonescu CM, Chang TC, Mendell JT, Salzberg SL (2015) StringTie enables improved reconstruction of a transcriptome from RNA-seq reads. Nat Biotechnol 33:290–295

Rogers K, Chen X (2013) Biogenesis, turnover and mode of action of plant microRNAs. Plant Cell 25:2383–2399

Sauter M (2015) Phytosulfokine peptide signaling. J Exp Bot 66:5161–5169

Shivram H, Le SV, Iyer VR (2019) MicroRNAs reinforce repression of PRC2 transcriptional targets independently and through a feed-forward regulatory network. Genome Res 29:184–192

Shukla LI, Chinnusamy V, Sunkar R (2008) The role of microRNAs and other endogenous small RNAs in plant stress responses. Biochim Biophys Acta 1779:743–748

Song X, Li Y, Cao X, Qi Y (2019) MicroRNAs and their regulatory roles in plant-environment interactions. Annu Rev Plant Biol 70:489–525

Srivastava R, Liu JX, Howell SH (2008) Proteolytic processing of a precursor protein for a growth-promoting peptide by a subtilisin serine protease in Arabidopsis. Plant J 56:219–227

Stuhrwohldt N, Dahlke RI, Steffens B, Johnson A, Sauter M (2011) Phytosulfokine-alpha controls hypocotyl length and cell expansion in *Arabidopsis thaliana* through phytosulfokine receptor 1. PLoS ONE 6:e21054

Tsukagoshi H (2016) Control of root growth and development by reactive oxygen species. Curr Opin Plant Biol 29:57–63

Voinnet O (2009) Origin, biogenesis, and activity of plant microRNAs. Cell 136:669–687

Willmann MR, Poethig RS (2007) Conservation and evolution of miRNA regulatory programs in plant development. Curr Opin Plant Biol 10:503–511

Yang H, Matsubayashi Y, Nakamura K, Sakagami Y (1999) Oryza sativa PSK gene encodes a precursor of phytosulfokine-alpha, a sulfated peptide growth factor found in plants. Proc Natl Acad Sci USA 96:13560–13565

Yu L, Liu Y, Liu Y, Li Q, Tang G, Luo L (2016) Overexpression of phytosulfokine-α induces male sterility and cell growth by

regulating cell wall development in *Arabidopsis*. Plant Cell Rep 35:2503–2512

Zhao XY, Hong P, Wu JY, Chen XB, Ye XG, Pan YY, Wang J, Zhang XS (2016) The tae-miR408-mediated control of *TaTOC1* genes transcription is required for the regulation of heading time in wheat. Plant Physiol 170:1578–1594